Cappuyns V., Van Campen A., Helser J. (2021). **Antimony leaching from soils and mine waste from the Mau Due antimony mine, North-Vietnam,** Journal of Geochemical Exploration 220, 106663 https://doi.org/10.1016/j.gexplo.2020.106663

Antimony leaching from soils and mine waste from the Mau Due antimony mine, North-Vietnam

Valérie Cappuyns[1,2,*], Axelle Van Campen[2], Jillian Helser[1,2]

[1] Center for Economics and Corporate Sustainability (CEDON), KU Leuven, 1000 Brussels, Belgium

[2]Department of Earth and Environmental Sciences, KU Leuven, 3001 Leuven, Belgium

[*]Corresponding author. Tel: +32 2 608 1453, E-mail: valerie.cappuyns@kuleuven.be

Abstract

Antimony (Sb) is an element with a growing concern due to its toxicity, but also because of its criticality. While the impact of Sb mining is documented in literature from China and Europe, still little data is available concerning the environmental impact of Sb mining in Vietnam. This paper presents the results of an exploratory study of mine waste and soil samples from the Mau Due mine (North Vietnam). The chemical and mineralogical composition of the samples was determined as well as the water-soluble and exchangeable/reversibly adsorbed Sb species, and the release of Sb at different pH values was investigated. Antimony concentrations in the mine waste samples (slags and waste rock) were in the range of 186-27221 mg/kg, while soils were characterized by Sb concentrations in the range of 47-95 mg/kg. In one mine waste sample, the primary mineral stibnite was found. The investigated mine waste samples also contained pyrite, which was not found in the soil samples. The leaching of Sb from all the samples with water was relatively low, as less than 1% of the total Sb content in the samples was released. In absolute values, this resulted in water-extractable Sb concentrations (24 h extraction) up to 430 µg/l, except for an alkaline slag sample, which released 23.5 mg/l of Sb, and the mine waste samples containing stibnite (2.9 wt.%), which released 16.6 mg/l of Sb. Based on the outcomes of this reconnaissance study, recommendations for further investigation of the waste heaps around the mine were made, taking into account the protection of health and the environment, and the sustainable management of secondary (waste) resources.

Keywords: antimony; leaching; soil; mining waste

1. Introduction

Antimony (Sb) is an element with a growing concern due to its toxicity, but also because of its criticality. Antimony was identified as one of 27 critical raw materials for the European Union (European Commission, 2017). Antimony is the 9th most commonly mined element, and has several industrial applications, such as in flame retardants, batteries, weapons, etc. (Alloway, 2013). China is by far the most important producer of Sb in the World (with an Sb production amounting to approximately 100 000 metric tons in 2019), followed by Russia and Tajikistan (Statista, 2019). The world's annual production is around 163 ktons of Sb, mostly in China, while it is no longer mined in EU countries (Deloitte sustainability, 2015). Antimony ores are generally processed into Sb metal by mining companies, mainly outside of the EU. Around 50 tons of Sb is processed in the EU from Sb ores and concentrates that are imported and about 11 000 tons of Sb metal is recovered from secondary material (waste, scrap and ash residues containing Sb) (Deloitte Sustainability, 2015).

Antimony toxicity mainly occurs due to occupational exposure and may cause respiratory irritation, pneumoconiosis, Sb spots on the skin and gastrointestinal symptoms (Sundar and Chakrvarty, 2010). According to the International Agency for Research on Cancer, antimony trioxide can be carcinogenic to humans (group 2B) and antimony trisulfide is not classifiable as to its carcinogenicity (group 3) (ATSDR, 2017).

Antimony is a metalloid with atomic number 51, with a high affinity for heavy metals (e.g. Fe, Cu, Pb), and sulfur. Average Sb concentrations in rocks and soils are in the range of 0.15-2 mg/kg and 0.3-8.6 mg/kg, respectively (Pierart et al. 2015). In mine waste, and in soils in the vicinity of mines, much higher Sb concentrations are usually found (Okkenhaug et al., 2011). More than a hundred Sb-minerals occur on Earth (Anderson, 2012). Antimony is found as a major element in many primary minerals, stibnite being the most common Sb-sulfide (Roper et al., 2012). Dissolution of stibnite (Sb_2S_3) in oxidizing conditions releases Sb, and Sb is incorporated into the mineral structures of several secondary minerals. The most commonly formed secondary Sb(V) minerals are Sb-bearing Fe hydroxides (goethite (α-FeOOH) and lepidocrocite (γ-FeOOH)), together with Sb-bearing jarosite ($KFe_3(SO_4)_2(OH)_6$) and Sb(-Fe)oxides and hydroxides such as tripuhyite ($FeSbO_4$), senarmontite (Sb_2O_3), romeite ($Ca_2Sb_2O_6OH$), cervantite (Sb_2O_4), kermesite (Sb_2S_2O), and valentinite (Sb_2O_3) (Courtin-Nomade et al., 2012). Antimony is also a component of coal and petroleum (Alloway, 2013). The primary mineral, stibnite, mainly occurs in mineralizations and quartz (SiO_2) veins. Metalliferous ore mining and smelting industries are currently the main sources of Sb pollution (He et al., 2019).

Antimony occurs in the environment in four oxidation states (−III, 0, III, and V) with Sb(III) and Sb(V) being the most frequently occurring species. The oxidation state also determines the toxicity of Sb, which decreases in the following order: Sb(III) > Sb(V) > organoantimonials. Microbial transformations catalyze the conversion of one Sb species into another (Mitsunobu et al., 2006; Lehr et al., 2007). At natural pH values, Sb is present as soluble $Sb(OH)_6^-$ in oxic systems and as soluble $Sb(OH)_3$ in anoxic ones at natural pH values. Under reducing conditions, and in the presence of sulfur, stibnite, $Sb_2S_3(s)$, is formed at low to intermediate pH values. At higher pH values, the SbS_2^- species replaces stibnite (Filella et al., 2002a). In soils, $Sb(OH)_6^-$ represents the major species over a wide Eh range (Mitsunobu et al., 2006).

pH and microorganisms are key parameters in biogeochemical cycling of Sb through the dissolution and oxidation of Sb-sulfide and the formation of secondary Sb(V)-bearing minerals (Loni et al. 2020).

Fe(hydr)oxides play an important role in the sorption and incorporation of Sb(V) and Sb(III). Johnston et al. (2020) found a strong association between Sb and poorly-crystalline Fe(III) mineral phases such as ferrihydrite (Fe_2O_3)•$0.5H_2O$). They also found evidence that As(V) was more strongly retained in the solid phase than Sb(V) in an oxic river system. Sb(V) adsorbs strongly to the surface of goethite and is also readily incorporated into the goethite structure during recrystallization (Burton et al., 2020). At very high aqueous Sb concentrations and near-neutral pH conditions, tripuhyite, is formed, a highly stable Fe(III)−Sb(V) oxide (Burton et al., 2020). Adsorption of Sb(III) to the surface of goethite is rapidly followed by electron transfer from surface-complexed Sb(III) to structural Fe(III), resulting in the formation of Sb(V) and Fe(II), forming tripuhyite (Belzile et al., 2001; Leuz et al., 2006). Pyrite can also contain a wide range of trace elements, which includes Sb (Li et al. 2018). Sorption of Sb(III) and Sb(V) to Fe(hydr)oxides and kaolinite is greatly influenced by pH, with increased sorption as pH decreases, and desorption as pH increases towards alkaline conditions (Guo et al., 2014a; Rakshit et al., 2015).

The effect of soil organic matter (SOM) on the mobility of Sb is somewhat ambiguous. On the one hand, SOM is reported to decrease Sb availability to plants by making stable complexes of Sb-humic acid (Steely et al., 2007). On the other hand, several authors (Clemente et al., 2010; Nakamaru and Peinado, 2017) showed that the application of compost to contaminated soil increased Sb in soil pore water, while Sb uptake by plants did not systematically increase. In waterlogged soils, Verbeeck et al. (2020a) found a decrease in Sb mobility at high Sb concentrations and an increase in Sb mobility at low Sb concentrations, which was largely determined by the electron donor capacity of SOM. In oxidizing conditions, $Sb(OH)_6$ mobility also increased with increasing SOM at low soil Sb concentration, which was explained by competitive sorption on Fe and Al hydroxides (Verbeeck et al. 2019).

While the occurrence of Sb in the environment is well documented in literature from China (e.g. He, 2007), Europe (e.g. Álvarez-Ayuso et al., 2012; Courtin-Nomade et al., 2012; MacGregor et al., 2015), and Australia (e.g. Johnston et al., 2020; Radková et al., 2020), little data are available concerning the environmental impact of Sb mining in Vietnam (Isuhara and Xian, 2013). This paper presents the first published geochemical leaching characterization data of mine waste, soil and slag samples from the Mau Due mine, in North Vietnam. Mining activities in Vietnam are important for the development of the country. However, mining also causes a loss of natural resources and has a serious impact on the environment (Vu et al., 2012).

This research is an exploratory study of mine waste from the Mau Due mine, and slag and soil samples from the Sb refinery, and is not intended to map the Sb contamination in the area. Besides providing data concerning the chemical and mineralogical composition of mine waste and soils at the Mau Due mine, the release of Sb is also investigated, under different conditions. Based on the results, a first estimate of the potential risks related to the mining activities and waste disposal is made, with the aim to provide recommendations for further investigation and characterization of the mining waste and slag heaps, in view of more sustainably managing the mining site. Although we were most interested in the release of Sb from the soil and mine waste samples, we also determined the total elemental concentrations, in order to have a reference for comparison with other studies and with guideline values.

2. Materials and methods

2.1 Site description

The Mau Due mine is located in the province of Ha Gian, at a latitude of 23° 4' 44'' North & longitude 105° 14' 52'' East in a mountain region in northern Vietnam (Figure 1), close to the Chinese border and to the In-bearing Sn-Pb-Zn deposits of Du Long mine, China (Ishihara et al., 2011).
The Songhien formation is the most important host rock of the Mau Due Sb ore body. It is composed of sandstones, black shale and sericitic shale and has a thickness of about 300 m (Xuan, 2011). The Mau Due Sb deposit is a small fracture filling-type Sb deposit (Ishihara and Xuan, 2013). Three ore bodies extend discontinuously in the North East – South West direction. The main ore body is located in the central part of the area and has a total length of 1300 m (North East – South West direction). These orebodies are mostly composed of quartz (20-70 %) and small amounts of calcite ($CaCO_3$). The ore minerals are stibnite, and very small amounts of pyrite (FeS_2), arsenopyrite

(FeAsS), sphalerite ((Zn, Fe)S), and berthierite ($FeSb_2S_4$) (Ishihara and Xuan, 2013). The average Sb content in the ore ranges from 3.13 to 12.03% (Xuan, 2011).

Besides the primary ore mineral stibnite, secondary Sb-containing minerals are found, which were formed by the weathering of stibnite (Sb_2S_3): valentinite and lewisite ($CaSb_2O_5(OH)_2$) (Ishihara and Xuan, 2013).

In 1993, exploitation of the ore body was initiated by open-pit mining. A refinery was installed in 2002. Since 2002, the annual Sb production of the mine amounts to 100 tons (Ishihara and Xuan, 2013), which is a substantial part of the total Sb production in Vietnam, which reached approximately 576 tons in 2017 (Doan, 2020).

The climate in this region is subtropical, with cool winters. The coolest month is January with an average temperature of 15°C, and the average temperature in August is 29°C. The average annual precipitation in Ha Gian province is 2492 mm (source: climate-data.org)

2.2 Sampling of slag, mine waste and soils

Samples were collected in January 2015, using a stainless steel shovel. Eight different samples were taken (Figure 1):

- Five mine waste samples, taken from the waste heaps in the center of the area. In the central part of the mining area (Figure 1), surface samples of the mine waste (samples SH1, SH2, SH3, SH4, and SH5) were taken along a transect, 150 m apart. The samples were taken as composite samples, composed of 5 sub-samples, collected in a star-like pattern (Ganne et al., 2006). Since the aim of the study was not to completely map the mining area, but rather to obtain a preliminary idea of Sb concentrations in the area, a limited amount of samples were taken. Moreover, access to the mine was restricted because it is still operational.
- One slag sample (SL1) of ± 1 kg, sampled from a waste heap next to the ore treatment facility. As this was a preliminary study, we were only allowed to take one sample from the slag heap. This sample is not representative of the slag heap. However, for follow-up studies, a more detailed sampling will be performed, but the present study gives an example of characterization methods that can be applied.
- Two soil samples (SO1 and SO2), collected in the vicinity of the slag heap. Soil samples were also taken as a composite sample. Again, this will not allow for mapping of the Sb contamination in the area, but gives a preliminary indication of Sb concentrations in soils close to the slag heap. The geochemistry of soil and stream sediments around the Mau Due stibnite deposit has already been investigated (Ishuara and Xuan, 2013), but not the soils nearby the Sb refinery.

Figure 1 here

The samples were air-dried, and sent to KU Leuven (Belgium) for analysis. Soil and mine waste samples, which all consisted of fine-grained material, were disaggregated in a porcelain mortar. The slag sample was first crushed with a hammer, and then further ground with mortar and pestle.

2.3 Sample digestion for chemical characterization

Two different dissolution methods were applied to the eight samples: hot plate digestion in which 4 strong acids were used to dissolve the sample, and a fusion method with lithium borate ($LiBO_2$). Each sample was digested in duplicate (by both methods), and two blanks and a certified reference material (GBW-7411) (Supplementary material, Table S1) were also included.

2.3.1 Multi acid digestion method

The total element concentrations in the samples were determined with a multi-acid digestion procedure using 4 acids (HNO_3 (nitric acid), $HClO_4$ (perchloric acid), HF (hydrofluoric acid) and HCl (hydrochloric acid). Fifty mg of sample was put in a Teflon beaker, together with 1.5 ml of concentrated HNO_3, covered and left under the fume hood for 2 days. After 2 days, the Teflon beakers were placed on a hot plate and heated at 140°C. Subsequently, the beakers were uncovered, and the temperature was increased to 200°C to evaporate the HNO_3. When the mixture was almost dry, 1 ml of concentrated $HClO_4$ was added to the beaker (covered with a loose cap) and heated at 200°C until almost dry. Next, 20 ml of concentrated HF were added to the beaker and heated at 240°C until completely dry. Finally, the residue in the beaker was dissolved by adding 20 ml of 2.5 mol/l HCl and put on a hot plate until the solid particles were entirely dissolved in the acid solution. The solution was filtered by a Whatman filter and diluted to 50 ml with Milli-Q water.

2.3.2 Lithium borate fusion

Fusion is a method where an oxidized sample is dissolved in a molten flux at temperatures of around 1050°C. Lithium metaborate ($LiBO_2$) is mixed with the sample and heated until the lithium borate melts and dissolves the sample to form a homogenous mass. The resulting solid is dissolved in acid for analysis. One hundred mg of sample was added to 500 mg of $LiBO_2$, in a graphite crucible and heated for 10 min at 1000°C in a muffle furnace, which resulted in the generation of a melt phase ($LiBO_2$ pearl). This $LiBO_2$ pearl was poured into 50 ml of HNO_3 (0.42 mol/l) and stirred on a magnetic stirrer to dissolve the $LiBO_2$ pearl. After 10 min, the pearl was dissolved and the solution was poured into a 50-ml plastic bottle. All measurements were made against calibration curves of five known reference materials which underwent lithium metaborate fusion sample preparation.
The solutions of both methods were analyzed for major and trace elements by ICP-OES (Varian-720 ES). Before measurement, the solutions were diluted by a factor 10 with Milli-Q water (see Section 2.5).

2.4 Mineralogical sample characterization

All samples were analyzed with XRD (X-ray diffraction). For the XRD identification, a subsample was wet ground (5 min) by a miller (McCrone Micronizing) using 5 ml of ethanol as a grinding agent. For quantification, an internal standard was added (i.e., 0.2 g of zincite was combined with 1.8 g of sample). After being ground, the sample was recuperated in porcelain cups and dried for 1- 2 days under a fume hood. Then, dried samples were gently disaggregated in an agate mortar and passed through a 250 µm sieve. Sample holders were gently tapped while filling, to ensure good packing of the grains. A Philips PW1830 diffractometer with Bragg/Brentano θ–2 θ setup, CuKα radiation, 45 kV

and 30 mA, graphite monochromator was used. Mineral phases were identified with the Profex 4.0 software, using the Rietveld refinement method for quantification (Bergmann et al., 1998).

2.5 Leaching tests

Leaching tests were performed on all samples with different extraction solutions. The first two extractions were based on the work of Ettler et al. (2007), who used an extraction with demineralized H_2O (DW) and with $Na_2HPO_4.2H_2O$ 0.1 mol/l to quickly investigate the water-soluble and exchangeable/ reversibly adsorbed Sb fraction. The influence of alkaline pH on the mobility of Sb was assessed further by means of extractions with diluted Na solutions, with concentrations varying between 0.005 mol/l and 0.1 mol/l NaOH.
Additionally, the EN 12457-2 test was performed according to the guidelines of the European Committee for Standardization (CEN). It specifies a compliance test providing information on leaching of granular wastes and sludges under the experimental conditions and is used to classify waste materials in the EU (EN 12457-2, 2002).
1 g of each sample was weighed in a polyethylene centrifuge tube. In each tube, 10 ml of extraction fluid was added, and the tubes were fixed on a horizontal shaking device (Edmund Buhler Gmbh) and shaken for 2 or 24 h (see Table 1 for the operational parameters). After centrifugation (15 min., 3000 rpm, Beckman G6 centrifuge), the solution was separated from the solid sample, and the pH of each solution was measured with a Hamilton Single Pore Glass pH-electrode. Before ICP-OES analysis, the solutions were filtered (0.45 µm).

Table 1 here

2.6 Analyses of digests and leachates

Elemental concentrations (Al, Ca, Fe, K, Mg, P, S, Sb, As, Cd, Co, Cr, Cu, Mn, Mo, Ni, Pb and Zn) in the digests and the leachates were measured by ICP-OES (Varian 720ES).
Calibration solutions were prepared from certified multi-element ICP standard stock solutions and from Plasma HIQU single element solutions from CHEM-LAB (Belgium). Blanks were also included in the calibration. All solutions were prepared from 18 MΩ/cm^3 ultra-pure water supplied from a millipore system and stabilized with ultra-pure nitric acid (CHEM-LAB). Each measurement was carried out with three replicates.
Speciation-equilibrium calculations were performed with the computer program PHREEQC (Parkhurst and Appelo, 1999), with the database minteq.v4.dat (Gustafsson, 2013), and using specific reactions for Sb phases from Majzlan et al. (2016).

3. Results

3.1 Total element concentrations and mineralogy

Very high Sb concentrations, up to 15 700 mg/kg were measured in the slag sample, as well as in some mine waste samples (Table 2). Mine waste samples SH3, SH4, and SH5, show moderate Sb-

concentrations. Both soil samples (SO1 and SO2) are clearly contaminated with Sb, but concentrations are much lower than in the slag and mine waste. Heavy metals such as Cr, Cu, Pb, and Zn did not display particularly high concentrations (Table 2). In the discussion section, most attention will go to Sb, as this is the main metal(loid) in the samples. Occasionally, results for As will also be briefly discussed.

Table 2 here

Quartz (23-46 wt.%), clay minerals (2.4-7.8 % wt.%), micas (20-49% wt.%) and gypsum (0.8-8.1% wt.%) were the main minerals in all mine waste samples (SH1 to SH5), except in sample SH1 and SH2, where respectively 26% and 21% of dolomite ($CaMg(CO_3)_2$) was also present. These were also the only samples containing calcite ($CaCO_3$, resp. 0.7 and 2.5 wt.%). Stibnite was the only Sb-bearing mineral found in one of the mine waste samples (sample SH2). The mine waste samples also had 0.9-3.9 % of pyrite.
In the slag sample (SL1), quartz was the main mineral, next to cristobalite (polymorph of quartz), calcite ($CaCO_3$), and augite ($(Ca,Na)(Mg,Fe,Al,Ti)(Si,Al)_2O_6$). A Sb bearing minerals, namely cervantite (0.7 wt.%) was also detected.
Quartz, clay minerals (illite and kaolinite), and micas were the main minerals found in the soil samples, with small amounts of feldspars, augite and goethite (Supplementary material, Table S2).

3.2 Leaching tests

The extractions with water and with the 0.1 mol/l $Na_2HPO_4.2H_2O$ solution, showed high variability with respect to the leaching of elements, and the pH of the extracts (Figure 3). From 0.06 to 1.7% of the total Sb content of the samples was extracted with water ('water-soluble Sb'), and 0.1 to 2.5 % with the phosphate solution ('reversibly/exchangeable Sb'). The diluted 0.005, 0.01 and 0.1 mol/l NaOH solutions extracted more Sb as the OH- concentrations increased, which was expected based on the occurrence of Sb as anionic species. The pH of the 0.005 mol/l NaOH extract was in the range 2.6-10.9 after extraction, pointing to a different base neutralization capacity of the different samples. With the 0.01 mol/l NaOH solution, the pH after extraction was in the range 7.1- 11.8. The pH of the extract after extraction with 0.1 mol/l NaOH was comparable for all samples, namely 12.9 ± 0.1.

Figure 2 here

4. Discussion

4.1 Comparison between sample digestion techniques

In general, the determination of Sb in solid samples such as waste, soils and sediments received less attention than the determination of Sb in water samples, where the speciation of Sb has also been a frequently addressed research topic (e.g. Kumar and Riyazuddin, 2007; Hasanin et al., 2016). Many

different methods have been used for the determination of total or pseudo-total concentrations of Sb in soils, sediments, and waste materials. An overview of studies dealing with the determination of Sb in (mining) waste samples is provided in Table 3. With respect to destructive methods, acid digestion methods are most often used, using different combinations of acids and either a hot plate or a microwave to digest the samples (Table 3). Pseudo-total Sb concentrations are often determined by aqua regia destruction, but sometimes other, more aggressive, acid digestion techniques are used.

The recovery of Sb concentrations from environmental samples depends on the extraction method chosen (Hjortenkrans et al., 2009). Therefore, the choice of reagents for sample digestion requires careful consideration to ensure adequate matrix dissolution and prevent the formation of insoluble Sb-bearing precipitates (Nash et al., 2000). Most acid dissolution methods do not completely dissolve the solid samples and provide 'pseudo-total', or 'near-total' concentrations of Sb. Tighe et al. (2004) compared open hot plate digestion and microwave digestion methods with nitric acid or aqua regia to determine near-total Sb concentrations in a contaminated floodplain and found that the aqua regia microwave destruction method performed better in terms of reproducibility than a nitric acid digestion method (microwave and hot plate).

Only a few studies using non-destructive techniques were found in published literature. Instrumental Neutron Activation Analysis (INAA) (Murciego et al., 2007) and X-ray fluorescence (XRF) (Marriussen, 2012) were used to measure Sb concentrations, respectively floodplain soils and in soils from a firing range. XRF is less suitable for Sb analysis, especially in organic-rich soil, but may be used on powdered mineral soil if the concentration is higher than 50 mg/kg (Mariussen 2012).

In the present study, two digestion methods, namely a hot plate multi-acid digestion and a lithium metaborate fusion were performed, and the performance of both destruction techniques were compared (Figure 3). Fusion involves the complete dissolution of the sample in a melt (molten) flux. Fusions are generally more aggressive than acid dissolution methods. A disadvantage is that there can be a loss of volatile elements (e.g., As, Pb, Sb) during this type of digestion. The multi-acid digestion uses a combination of 4 concentrated acids: HNO_3, $HClO_4$, HF and HCl. HCl is known to dissolve silicate, iron and sulfide minerals, especially at elevated temperatures and pressures (Pahlavapour et al., 1980; Kammin and Brandt, 1988). Tighe et al. (2005 a, b) showed that iron oxyhydroxides, silicates, and sulfide phases often play an important role in the binding of Sb. The use of concentrated HNO_3 is necessary for the digestion of soil samples to release Sb from any organic matter. HF dissolves silicate minerals, but some refractory minerals (especially oxide minerals) are only partially digested. Therefore, the multi-acid digestion used in this study can be considered a near-total digestion.

Table 3 here

The incomplete dissolution of the samples by the multi-acid digestion method can be deduced from the comparison with the $LiBO_2$ fusion method (Figure 3). For most major elements, such as Fe, Al, K, Mg, higher concentrations are obtained with the $LiBO_2$ fusion method than with the multi-acid digestion method (Figure 2 for Fe), which is most likely related to the incomplete dissolution of the slag material by the multi-acid digestion. For heavy metals and metalloids, the difference between both digestion methods is less pronounced. Only for the slag sample (SL1), much more Sb was

326 measured with the $LiBO_2$ method (27 221 mg/kg), than with the multi-acid digestion method (11 522
327 mg/kg) (Figure 2), pointing to the incorporation of Sb in phases that are resistant to the multi-acid
328 digestion. Fe-minerals, such as goethite, ferrihydrite, and tripuhyite can act as sinks for Sb (Karimian
329 et al., 2018; Radková et al., 2020), but are most likely dissolved by the acid digestion. Refractory Fe-
330 minerals in the slag, however, were not dissolved by the multi-acid digestion.
331 For the soil samples, concentrations of Sb are comparable with both methods. Telford et al. (2008)
332 compared Sb extracted with a multi-acid dissolution method (using the same 4 acids as in the
333 present study). Antimony concentrations extracted from contaminated soils by the 1:2 (v/v)
334 HNO_3:HCl acid mixture at 150 °C were similar to Sb extracted by the four acid mixture. In what
335 follows, we will use the results of the multi-acid digestion for metalloids (including Sb), heavy metals,
336 and S, and the results of the $LiBO_2$ fusion for major elements (Table 2).
337
338 ***Figure 3 here***
339

340 ## 4.2 Sb in mine waste

341 In the present study, both mine waste samples with rather low and with very high Sb concentrations
342 were found. Guo et al. (2014b) found Sb concentrations of 6930 and 11100 mg/kg in water resp.
343 quenched and desulfurized slags produced in the smelting processes in the Xikuangshan area.
344 Tailings and slag residues from an old Sb mine of the French Massif Central have been reported to
345 have concentrations of Sb in slags and tailings of 1700 and 5000 mg/kg, respectively (Courtin-
346 Nomade et al., 2012).

347 Stibnite in mesothermal vein deposits of eastern Australia and southern New Zealand is oxidized
348 under humid to semiarid conditions and transforms to oxides including valentinite, senarmontite,
349 and stibiconite ($Sb^{3+}Sb^{5+}_2O_6(OH)$. Oxidation of stibnite and associated arsenopyrite and pyrite causes
350 local acidification, which is readily neutralized by carbonates in mineralized zones and host rocks.
351 Stibnite dissolves readily in moderately oxidized waters (SbO_3^-), with the formation of Sb oxide, and
352 Sb sorption/coprecipitation with amorphous iron oxyhydroxides (Ashley et al., 2003). Secondary Sb
353 minerals are most likely formed in the immediate vicinity of the oxidizing primary mineral (Diemar et
354 al., 2008). At very high aqueous Sb concentrations and near-neutral pH conditions, tripuhyite is
355 formed, a highly stable Fe(III)−Sb(V) oxide (Burton et al., 2020).

356 Samples SH2 still contains stibnite and pyrite, indicating that it is not (fully) oxidized yet. In the slag
357 sample, cervantite was found, the oxidation product of stibnite that is is often encountered in the
358 stibnite oxidation zone (Ashley et al., 2003).

359 High variability was observed with respect to the pH of the mine waste samples. Whereas sample
360 SH1 and SH2 displayed a neutral pH, samples SH3 and SH5 were moderately acidic, and sample SH4
361 even very acidic (Table 3). These observations suggest that sample SH4 is older, and already
362 underwent weathering, producing acid mine drainage, while mine waste with a neutral pH and
363 slightly acidic pH still contains some carbonates, which can buffer acidity produced by the oxidation
364 of sulfides. The samples with a neutral pH (SH1 and SH2) indeed contained dolomite and carbonate,
365 whereas these minerals were not found in the other mine waste samples.

366 No relationship was however found between the S-, and Ca- content of the samples, and the pH. The
367 slag sample in this study (SL1) is Si-rich slag, with a low Fe content, and an alkaline pH. It is

368 characterized by a high Sb content (1.15 wt.%), but low concentrations of As and heavy metals
369 (Table 2).

370 Antimony is listed among the 27 critical raw materials for the EU (European Commission, 2017). In
371 view of resource protection, the potential for recovery of Sb from the mine waste and slags,
372 considering it as a secondary resource, should be investigated. This asks first of all for a more
373 detailed mapping and characterization of the mine waste and slags at Mau Due, in order to more
374 exactly know where highly concentrated waste materials can be found on the site, and estimate how
375 much of these materials are available. Based on that information, the recovery of Sb from mine
376 waste and slags could be considered. In a review on the recovery of Sb from end-of-life products and
377 industrial process residues, Dupont et al. (2016) pointed out that residues from the processing of
378 metal ores with high contents of Sb are currently discarded or stockpiled, causing environmental
379 concerns. Technologies for Sb recycling are available, but upscaling of these methods is necessary,
380 taking into account economic feasibility as well as environmental issues.

381 ## 4.3 Sb in soils

382 High concentrations of Sb and other heavy metals and metalloids are usually not limited to the
383 waste materials stored on mining sites themselves. Soils and sediments, as well as ground and
384 surface water in and around the mining and smelting sites also suffer from pollution. Several studies
385 on metallic pollution arising from the mining of Sb-ores, as well as dry fallout/fly ash and solid waste
386 from smelters have been conducted in the proximity of mining and metallurgical sites. Sometimes
387 samples were taken on the mining site itself, or in the broader mining area, including soils in the
388 neighborhood of the site (Table 3). Yuan et al. (2017) found concentrations in the range of 289–3100
389 mg/kg in soils flooded by smelting wastewater from a former stibnite, antimonite ($FeSb_2S_4$) and
390 plagionite ($Pb_5Sb_8S_{17}$) smelter. In literature (Table 3), mining-impacted soils with Sb concentrations
391 up to 11798 mg/kg have been reported (Okkenhaug et al., 2011).

392 In soil samples taken nearby (up to 1 km from the mine) the Sb mine of the Xikuangshan Sb deposit,
393 in which stibnite (Sb_2S_3) is the only ore mineral, has Sb levels ranging from 101 to 5045 mg/kg (He,
394 2007). Ishara and Xuan (2013) report that the pollution of soils and sediments due to As and base
395 metals around the Mau Due stibnite deposits was “weak”, with an average Sb concentration of 932
396 mg/kg in the soil in the wet season, and 342 mg/kg of Sb in the dry season. The Sb content of stream
397 sediments are much higher (average of 2536 mg/kg in the wet season and 2504 mg/kg in the dry
398 season). The soil samples analyzed in the present study were taken close to the smelter, and display
399 Sb concentrations which are comparable to the concentrations reported in Ishara and Xuan (2013).
400 Nevertheless, compared to Sb concentrations in soils not affected by mining and smelting activities,
401 which are of the order of a few mg/kg (Filella et al., 2002), these values cannot be considered ‘weak’,
402 and clearly carry the signature of the stibnite deposit and related mining and smelting activities in
403 the area.

404 Background values for Sb in soils have only been established in a few countries. In Cuba, the quality
405 reference value, based on the analysis of soils under natural conditions with little or minimal
406 anthropic interference, was established at 6 mg/kg for Sb (Alfaro et al., 2015). The background
407 values of Sb in Chinese soils are in the range of 0.8–3.0 mg/kg (Qi and Cao, 1991). In European soils,
408 (median of a dataset of resp. 783 and 840 samples) Sb concentrations are 0.47 mg/kg in subsoil and
409 0.60 mg/kg in topsoil. Enrichments of Sb in the soil are mainly related to ore deposits, and old

mining and smelting areas, with maximum values of 30.3 mg/kg in subsoils and 31.1 mg/kg in topsoils (Salminen et al., 2005). In a reconnaissance soil geochemical survey near Armidale, New South Wales (Australia), anomalous soil Sb levels (up to 150 mg/kg) were confined to within 100 m of known stibnite mineralization (Diemar et al. 2009). Several authors (Wilson et al., 2004; Diemar et al., 2009) state that the mobility of Sb in soils is quite limited such that Sb levels are confined to the immediate vicinity of the oxidizing Sb minerals.

Compared to the mine waste and slag samples, the soil samples (SO1 and SO2), taken in the vicinity of the smelter, were characterized by a lower Si-, Mn-, S- and Fe-content, but higher Mg- and Ca-concentrations (Table 2).
Arsenic is often found as a pollutant of Sb mining and smelting. However, we found a low to moderate enrichment of As in the mine waste and the soils, and there was no correlation between total As and Sb concentrations.

4.4 Water-soluble and reversibly sorbed/exchangeable Sb

The 0.1 mol/l Na_2HPO_4–extractable Sb concentration is used to estimate the "exchangeable" or "reversibly sorbed" Sb pool (Ettler et al., 2007). The 0.1 mol/l $Na_2HPO_4.H_2O$ solution resulted in slightly higher extractability of Sb compared to an extraction with water (Figure 2). However, this difference was not significant ($p > 0.1$). The soil samples SO1 and SO2 showed a low release of Sb with water (108 and 21 µg/l, respectively) and a slightly higher release with 0.1 mol/l $Na_2HPO_4.2H_2O$ (116 and 26 µg/l respectively), which represents 0.73 – 1.25% of the total content in the soil. It cannot be deduced from the results whether this is due to the effect of increasing phosphate concentrations or to the increase in pH. For the samples with a pH < 7 (SH3, SH4, SH5, SO1, and SO2), the pH of the phosphate extract was 2 to 4 units higher than the pH measured in water. For the samples with a pH > 7, this difference was less than 1 pH unit (Figure 2).

Antimony exists as either a neutral species or a negatively charged oxyanion. Phosphate ions can compete with Sb oxyanions bound to the surfaces of Fe(hydr)oxides, clay minerals and organic matter. Griggs et al. (2011) demonstrated the increased leaching of Sb in phosphate-treated soils compared to untreated control soils. Verbeeck et al. (2019), using a 0.1 mol/l $Na_2HPO_4.H_2O$ solution, extracted 1-4% of the total Sb in soil samples containing between 0.7 and 24 mg/kg Sb, and a varying SOM content. Ettler et al. (2007) also used an extraction with the same phosphate concentration as the present study, and reported a much more pronounced effect of phosphate on the mobilization of Sb, but the pH of the phosphate extract was also much lower than the pH obtained for our samples, pointing to a different pH buffering capacity of the soils. Similarly to our results, Park et al. (2018) reported that phosphate was not effective in the mobilization of an artificially contaminated soil (Sb_{tot} = 100 mg/g). They used a 0.02 mol/l phosphate solution, which is five times more diluted than the solution used in the present study. Whereas phosphate decreases Sb(V) adsorption on goethite, the influence of sulfate is minimal (Essington and Stewart, 2018). In a combined laboratory and field study, Rouwane et al. (2015) found that Sb release was favored under oxidizing conditions, particularly when dissolved organic carbon (DOC) increased in soil pore water (up to 92.8 mg/l). At laboratory-scale, Sb release was much higher under reducing conditions. The release of Sb PO_4^{3-}-enriched anoxic soils was probably induced by the combined competitive effect of hydrogen carbonates and phosphates for soil binding sites, pointing to the importance of the (alkaline) pH.

The low 'water-soluble' Sb fraction is in line with what has been reported for other soils impacted by Sb mining, despite the fact that most published results present data from closed mines.

Murciego et al. (2007) evaluated the water-soluble Sb fraction in mine soils (pH 4.3 – 7.2) following the DIN 38414-S4 (1984) procedure. This method uses deionized water, with a liquid: soil ratio of 1000 ml: 100 g, and a shaking period of 24 h, and is thus comparable to the EN 12457-2 test. The water-soluble fraction was in the range of 1-20 mg/kg, accounting for 0.13- 7.33 % of the total Sb content in the soils. The soluble Sb content in Scottish soils, determined with 1 mol/l NH_4NO_3 was on average 1.2% (range 0.01-8.8 %) in soils with an acidic to slightly acidic pH (Gál et al., 2007). The water extracts of topsoils from a polluted Sb smelting site in China contained 5.3-31.6 mg/kg of soluble Sb, which was 0.7–1.63% of the total Sb content in the soil (Sh et al., 2012).

To simulate the release of Sb from the soil at Su Suergiu (Italy), Cidu et al. (2014) performed batch tests with MilliQ water (L/S = 25 l/kg) using Sb-rich soil samples (4400 and 860 mg/kg) with a neutral pH. 1 to 6% of the total Sb content was released with water after 96 h.

Álvarez-Ayuso et al. (2012) reported soluble Sb ranging from < 0.01–0.779 mg/kg (EN 12457-2 test), which represented <1% of the total Sb content of the soils (with a pH ranging from 6.6 -8.0). All of these examples show that the mobility of Sb in soils, affected by mining, at acidic to slightly alkaline pH is rather low, with generally less than 10% of the total Sb content being released by water extraction. However, in absolute concentrations, sometimes very high Sb concentrations are found in the water extracts (e.g., 2.2 mg/l; Cidu et al., 2014, 12.9 mg/l; Murciego et al., 2007) of these highly contaminated mine soils.

There are no guideline values available for soluble heavy metal and metalloid concentrations in soils. As a reference, we could compare these water-soluble Sb concentrations in soils with values for surface and groundwater, and drinking water. In non-polluted waters, total dissolved Sb concentrations are usually less than 1.0 µg/l (Filella et al., 2002). According to the USEPA (2018), the maximum contaminant level for Sb in water was set at 6 µg/l for lifetime exposure of a 70 kg adult consuming 2 l of water daily. Guideline values for one-day and ten-days (10-kg child consuming 1 l of water per day) are reported as 10 µg/l. In Canada, the maximum acceptable concentration (MAC) for Sb in drinking water is set at 4 µg/l (Health Canada, 1999). In the European Union, a parametric standard for Sb is included in the EU Drinking Water Directive (EU, 1998), which equals 5 µg/l. The World Health Organization (WHO) has provided guidelines for drinking water quality of 20 µg/l (WHO, 2003), but some polyethylene terephthalate-bottled waters often contain higher levels of Sb when stored over an extended-time (2 weeks) in high-temperature (60°C) storage conditions (Carneado et al., 2015). The Sb content from water extraction of the soil samples (SO1 and SO2) are slightly above 20 µg/l. Despite the fact that this exceeds all guidelines for drinking water quality, we can still conclude that the solubility of Sb in the soils is rather low, which might be partly explained by the acid pH of the soils (pH 5.0 and 4.8), favoring the sorption of anionic Sb species.

For the mine waste samples, a longer extraction time (24 h vs. 2h) had a significant effect on the solubility of Sb, pointing to the importance of reaction kinetics (Figure 2). The European Union established guideline values, based on the EN 12457-2 leaching test (extraction with water at L/S 10 l/kg, 24 h), to classify waste as hazardous or non-hazardous waste. Based on these guidelines, only samples SL1 and SH2 exceed the guideline value for hazardous waste for Sb (Figure 3), while samples SH1 and SH4 also exceed the guideline value for non-hazardous waste.

Sb mobility is determined by many different parameters, and a comparison between different studies is not always straightforward. An important aspect here is also that the Sb-content of the mine waste is not always proportional to the amount of Sb released from the samples. Hu et al. (2016) even showed that the extent of Sb dissolution is negatively correlated with the Sb-concentration in the mineral phase. In the present study, the mine waste samples with the highest Sb content released between 1 and 2% of their total Sb content, while the samples with a lower total Sb content released less than 0.5 % of their total Sb content. The negative correlation between total and water-soluble Sb concentrations was thus not found in the present study.

With respect to other contaminants, water-soluble As-concentrations were in the range of 10-572 µg/l, with sample SH3 and SH4 exceeding the guidelines for non-hazardous waste. These two samples, with an acidic to strongly acidic pH (resp. 5.2 and 2.6), also displayed the highest release of Cd, Cr, Cu, Ni and Zn. However, the EU guidelines for hazardous waste were only exceeded for Ni and Cu (Supplementary material, Table S3).

4.5 Influence of pH on the release of Sb

The release of Sb increased towards more alkaline pH (Figure 4). The most prominent release was observed for the samples with the highest total content of Sb (SH2 and SL1, Table 2). Relative to the pseudo-total Sb concentration, most Sb was released from the mine waste samples (Figure 4, SH2, up to 14%; for the other mine waste samples, between 5 and 52 % of Sb was leached with the 0.1 mol/l NaOH solution), while only 3 % of the total Sb content was released from the slag sample (SL1) at pH 12 (which equals to 396 ± 10 mg/kg, Figure 4).

Figure 4 here

4.5.1 Sb release from soils

From the soil samples SO1 and SO2, resp. 17 and 2 % of the total Sb content was released with NaOH 0.1 mol/l. Serafimovska et al. (2013) used 0.1 mol/l of NaOH to isolate the soil fraction containing humic substances from soil samples, and found that between 6.1 and 13.7 % of the total Sb content was bound to soil humic acids. Using sorption experiments, Buschmann and Sigg (2004) showed that over 30% of total Sb(III) may be bound to humic acids. Steely et al. (2007) indicated that humic acids have a strong binding capacity for Sb, being able to immobilize it in the soil's organic layer. Besides the dissolution of humic acids at high pH, sorption of Sb(V) by humic acid also decreases as the pH increases.

The effect of soil pH on Sb mobility in soil is not always straightforward, and also depends on the redox status of Sb. In the pH range 2–11, Sb(III) exists as, $Sb(OH)_3$, a neutral complex, and Sb(V) exist as the negatively charged $Sb(OH)^-$ (Filella et al. 2002). $Sb(OH)_6$ is also the main Sb species over a wide range of Eh values in soil (Wilson et al. 2010).

Tighe et al. (2005b) reported a strong sorption capacity of amorphous Fe-oxides for Sb(V) in the pH range from 3–6.5. Humic acids can significantly contribute to the sorption of Sb(V) at these pH values. However, increasing soil pH can decrease the Sb holding capacity of humic acids, both for

Sb(III) and Sb(V) (Tighe et al., 2005b, Buschmann and Sigg, 2004). According to Casiot et al. (2007), Fe-oxides are considered as the main sorbing phase for Sb, and the mobility of Sb(V) in oxidizing conditions is higher than Sb(III) because of the smaller charge density and large ionic radius in the form of $Sb(OH)_6^-$. Antimony also strongly adsorbs onto clay minerals and hydrous Al-oxides (Ilgen and Trainor, 2012; Rakshit et al., 2015). It was not the aim of the present study to deduce the binding mechanisms of Sb onto soil components. However, based on the information about Sb occurrence in soil described above, the acidic pH values of the soil (pH 5.0 and 4.8) explain the low mobility of Sb. A substantial increase in the pH of the soils should be avoided, as this will result in the release of Sb. Recently, indications were found that Sb mobility increases upon aging of soils, suggesting that soils affected by historical contamination could have lower Sb mobility and bioavailability of Sb than recently contaminated soils (Verbeeck et al., 2020b). The Mau Due mine started its operations in 1993, and is still operational, resulting in both historical and new contamination. A better understanding of the factors affecting Sb mobility upon aging of soils would be useful to develop strategies to prevent Sb from migrating downwards to groundwater.
Arsenic is usually also found in the waste from Sb mining, and in soils contaminated by Sb mining and smelting. In addition, the geochemistry of Sb is often considered similar to that of As, although more recent studies (e.g. Fu et al., 2016) suggest that significant differences in mobility, bioavailability and bioaccumulation exist between As and Sb. The extraction with 0.01 mol/l of NaOH solution released respectively 5.2 and 22.5% of the pseudo-total As-content of soils SO1 and SO2. The release as a function of pH follows the same pattern as Sb (i.e., increased leaching as pH increases, Figure S1, Supplementary material), but proportionally less As is released from sample SO1. The natural co-occurrence of As with Sb, which are often believed to behave similarly, but which is definitely not always the case, offer an interesting further research opportunity for the soils and waste materials at the Mau Due mine.

4.5.2 Sb release from mine waste and slag

With respect to the mine waste and slag samples, the solubility of Sb-bearing minerals can also explain the leaching of Sb as a function of pH. The solubility of stibnite was modelled for sample SH2, for which the mineralogical analysis showed the occurrence of 2.9 wt.% of stibnite. Based on the total Sb concentration in this sample, this would mean that Sb entirely occurs as stibnite. The solubility of stibnite (taking into account an L/S ratio of 10 l/kg) was then modeled at the different pH values determined during the leaching tests with water and NaOH- solutions. Based on the modeling, stibnite completely dissolves at pH 7.5 and higher. However, other Sb-containing minerals are oversaturated at alkaline pH, with $Sb(OH)_3$ and Senarmontite (Sb_2O_3) displaying the highest saturation indices (Supplementary material, Table S4). However, when precipitation of the oversaturated minerals was included in the model, only $Sb(OH)_3$ precipitated. When we compare the amount of dissolved Sb as found experimentally, with the amount of Sb that would be dissolved according to the model (Figure 5a), we see that the dissolution and precipitation reactions alone are not sufficient to explain the pH-dependent release of Sb. At pH values 7.5 and 8.2, less Sb is found in solution than predicted by the model.

Besides stibnite, sample SH2 also contains clay minerals -and feldspars which can play a role in the sorption and desorption of Sb. At alkaline pH values, Sb occurs as a negatively charged species, which will desorb from negatively charged surfaces of clay minerals and feldspars. The Sb that is

578 released is apparently not precipitated as $Sb(OH)_3$, most likely because of slow reaction kinetics.
579 Besides mineralogy and pH, microorganisms also contribute to the dissolution of Sb-minerals, such
580 as stibnite, and thus contribute to the release of Sb(V) in groundwater and surface water (Loni et al.,
581 2020). The progressive (chemical and microbial) dissolution of stibnite, followed by microbial
582 oxidation to Sb(V) decreases the toxicity of Sb(III) to microorganisms. Moreover, Sb(V) can be
583 incorporated in goethite (Burton et al. 2020) or in Sb(V)-bearing mopungite ($NaSb(OH)_6$) (Multani et
584 al., 2016).
585 In the slag sample, modeling with PHREEQC indicates that the dissolution of cervantite increases
586 with increasing pH, but that Sb precipitates again as SbO_2. At pH values 9.5 and 10.6, a good fit
587 between the model and the experimental results is obtained when only dissolution of cervantite is
588 considered (without precipitation of SbO_2) (Figure 5b). However, at pH 12.1, the model predicts a
589 much higher release of Sb than is actually the case (experimental results), which indicates that Sb
590 most likely precipitates at pH 12.1. When precipitation is allowed in the model, Sb-concentrations
591 are underestimated by the model. This difference can be explained by slow precipitation and
592 reaction kinetics, Besides the dissolution and precipitation of Sb-bearing minerals, the desorption of
593 Sb from reactive surfaces (e.g. augite) might also play a role here
594 With respect to As, the release of As from the mine waste and the slag sample was very low, even
595 when the pH increased up to a pH of 11. At a pH > 12, 2 to 27% of the total As-content was released.
596 For the heavy metals, the pH increase resulted in a decrease of soluble concentrations.
597
598 ***Figure 5 here***

599 # 5. Conclusion

600 The present study shows that, when mine waste stored on the site of the Mau Due mine comes into
601 contact with water, it leaches up to 1.7% of its total Sb content. However, because of the high Sb
602 content of some of the materials (up to 2.7 wt.%), high dissolved Sb concentrations are found in the
603 leachates. Two of the investigated samples (SH2 and SL1) are listed by the EU as absolutely
604 hazardous waste, because of the leaching potential of Sb. Especially in the rainy season, leaching of
605 Sb from the mine waste and slags can contribute to the dispersion of Sb.
606 In all samples, an increased release of Sb was observed from pH 7.5 to 12.8. Modeling also indicated
607 that the dissolution of stibnite and re-precipitation as $Sb(OH)_3$ is not the only factor that explains Sb
608 solubility. Desorption reactions and the incorporation of Sb in mineral phases are most likely also
609 important factors in the retention and release of Sb from the waste materials and slags.
610 As long as the mine is operational, the release of Sb into the environment surrounding the mine (i.e.,
611 surface water, groundwater, soils and air) should be avoided. For the immobilization of Sb, several
612 pathways could be envisaged. Microorganisms can, under natural conditions, also decrease the
613 (mobile) Sb(V) concentration to some extent via the formation of secondary Sb(V)-bearing minerals
614 (Loni et al., 2020) or through incorporation in Fe(hydr)oxides such as goethite (Burton et al., 2020),
615 which offer new ideas about Sb(V) (bio)remediation.
616 However, immobilization of Sb is not sufficient to mitigate the risks posed by the uncovered waste
617 and slag heaps. The waste heaps consist of fine-grained material, that can be prone to wind erosion
618 in the dry season. Therefore, measures to prevent the further dispersion of Sb and other potentially
619 hazardous elements, both via wind erosion, should be put in place. In order to establish regulations
620 for environmental protection, it is necessary to raise governmental and public awareness. The high

concentrations of Sb imply an important potential hazard for soils, water bodies, and the food chain, for which appropriate measures are necessary.

Finally, two samples taken from the waste heaps showed Sb concentrations around 1-2 wt%. Further characterization of mine waste found within the mining site and the slags stored next to the refinery should give more detailed information on the chemical and mineralogical composition of the mine waste, as well as the heterogeneity in the composition. Based on the types (i.e., different mineralogical composition and Sb content) of mine waste found on site, an investigation on the feasibility of recovering Sb from these 'waste materials' is recommended.

Acknowledgments

We are grateful to Le Thi Thuy Van for taking the samples, Tom Vandermeeren for performing the extractions, and Elvira Vassilieva for carrying out the ICP-OES analyses. This work was financed with a KU Leuven Starting Grant (STG/14/010) of V. Cappuyns.

References

M.R. Alfaro, A. Montero, O.M. Ugarte et al., 2015. Background concentrations and reference values for heavy metals in soils of Cuba. Environ. Monit. Assess. 187, 4198. https://doi.org/10.1007/s10661-014-4198-3

B.J. Alloway, 2013. Heavy Metals in Soils. Vol. 22. Environmental Pollution. Dordrecht: Springer Netherlands.

E. Álvarez-Ayuso, V. Otones , A. Murciego, A. García-Sánchez, I. Santa Regina, 2012. Antimony, arsenic and lead distribution in soils and plants of an agricultural area impacted by former mining activities. Sci.Total Environ. 439, 35–43. http://dx.doi.org/10.1016/j.scitotenv.2012.09.023

C.G. Anderson, 2012. The Metallurgy of Antimony. Chem. Erde 72, 3–8. https://doi.org/10.1016/j.chemer.2012.04.001

P.M. Ashley, D. Craw, B.P. Graham, D.A. Chappell, 2003. Environmental mobility of antimony around mesothermal stibnite deposits, New South Wales, Australia and southern New Zealand. J. Geochem. Explor. 77, 1-14. https://doi.org/10.1016/S0375-6742(02)00251-0

ATSDR. 2017. Agency for Toxic Substances and Disease Registry. Toxicological profile for antimony. Atlanta, GA: U.S. Department of Health and Human Services, Public Health Service. Retrieved from http://www.atsdr.cdc.gov on 15 January 2019

N. Belzile, Y.W. Chen, Z. Wang, 2001. Oxidation of antimony(III) by amorphous iron and manganese oxyhydroxides. Chem. Geol. 174, 379−387.

J. Bergmann, P. Friedel, R. Kleeberg,1998. BGMN — a new fundamental parameter based Rietveld program for laboratory X-ray sources, its use in quantitative analysis and structure investigations. CPD Newsletter, Commission of Powder Diffraction, International Union of Crystallography 20, 5–8.

J. Buschmann, L. Sigg, 2004. Antimony (III) binding to humic substances: influence of pH and type of humic acid Environ. Sci. Technol. 38, 4535-4541. https://doi.org/10.1021/es049901o

E.D. Burton, K. Hockmann, N. Karimian, 2020. Antimony Sorption to Goethite: Effects of Fe(II)-Catalyzed Recrystallization. ACS Earth Space Chem.4, 476−487.

S. Carneado, E. Hernández-Nataren, J.F. López-Sánchez, A. Sahuquillo, 2015. Migration of antimony from polyethylene terephthalate used in mineral water bottles. Food Chem., 166(1), 544–550. https://doi.org/10.1016/j.foodchem.2014.06.041

C. Casiot, M. Ujevic, M. Munoz, J.L. Seidel, F. Elbaz-Poulichet, 2007. Antimony and arsenic mobility in a creek draining an antimony mine abandoned 85 years ago (upper Orb basin, France). Appl. Geoch. 22(4), 788-798. https://doi.org/10.1016/j.apgeochem.2006.11.007

R. Cidu, R. Biddau, E. Dore, A. Vacca, L. Marini, 2014. Antimony in the Soil–water–plant System at the Su Suergiu Abandoned Mine (Sardinia, Italy): Strategies to Mitigate Contamination. Sci Total Environ. 497–498, 319–31. https://doi.org/10.1016/j.scitotenv.2014.07.117

R. Clemente, W. Hartley, P. Riby, N.M. Dickinson, N.W. Lepp, 2010. Trace element mobility in a contaminated soil two years after field-amendment with a greenwaste compost mulch Environ. Pollut., 158. 1644-1651. https://doi.org/10.1016/j.envpol.2009.12.006

A. Courtin-Nomade , O. Rakotoarisoa , H. Bril H., M. Grybos, L. Forestier, F. Foucher M. Kunz, 2012. Weathering of Sb-rich mining and smelting residues: insight in solid speciation and soil bacteria toxicity Chem. Erde-Geochem., 72, 29-39. https://doi.org/10.1016/j.chemer.2012.02.004

G.A. Diemar, M. Filella, P. Leverett, P.A. Williams, 2009. Dispersion of antimony from oxidizing ore deposits. Pure Appl. Chem. 81, 1547-1553. https://doi.org/10.1351/PAC-CON-08-10-21

Deloitte Sustainability, 2015. Study of Data for a Raw Material System Analysis: Roadmap and Test of the Fully Operational MSA for Raw Materials. Prepared for the European Commission, DG GROW. ISBN 978-92-76-08568-3. Available at https://ec.europa.eu/jrc/en/scientific-tool/msa

E.Z. Doan. 2020. Antimony ore production in Vietnam from 2010 to 2018. May 11, 2020. Retrieved from https://www.statista.com/statistics/1003650/vietnam-antimony-ore-production/

D. Dupont, S. Arnout, P.T. Jones, K. Binnemans, 2016. Antimony Recovery from End-of-Life Products and Industrial Process Residues: A Critical Review. J. Sustain. Metall. 2, 79–103. https://doi.org/10.1007/s40831-016-0043-y

V. Ettler, M. Mihaljevič, O. Šebek, Z. Nechutný, 2007. Antimony availability in highly polluted soils and sediments – a comparison of single extractions. Chemosphere 68, 455-463. https://doi.org/10.1016/j.chemosphere.2006.12.085

EU, 1998. Council Directive 98/83/EC on the quality of water intented for human consumption. Adopted by the Council, on 3 November 1998.

European Commission, 2017. Study on the review of the list of Critical Raw Materials - Criticality Assessments. Directorate-General for Internal Market, Industry, Entrepreneurship and SMEs. Directorate Industrial Transformation and Advanced Value Chains Unit C.2 — Resource Efficiency and Raw Materials. Luxembourg: Publications Office of the European Union, 2017, https://doi/10.2873/876644

EN 12457-2, 2002. Characterisation of waste leaching compliance test for leaching of granular waste materials and sludges—part 2. The European Committee for Standardization (CEN), Brussels.

M. E. Essington, M.A. Stewart, 2018. Adsorption of Antimonate, Sulfate, and Phosphate by Goethite: Reversibility and Competitive Effects, Soil Science Society of America Journal, 82(4), 803-814). https://doi.org/10.2136/sssaj2018.01.0003.

EU, 1998. Council Directive 98/83/EC of 3 November 1998 on the quality of water intended for human consumption, ANNEX I: PARAMETERS AND PARAMETRIC VALUES, PART B: Chemical parameters". EUR-Lex. Retrieved 30 December 2019.

M. Filella, N. Belzile, Y.W. Chen, 2002. Antimony in the environment: a review focused on natural waters: I. Occurrence. Earth Sci. Rev., 57 (1–2), 125-176. https://doi.org/10.1016/S0012-8252(01)00070-8

H.C. Flynn, A.A. Meharg, P.K. Bowyer, G. I. Paton, 2003. Antimony Bioavailability in Mine Soils. Environ. Pollut. 124 (1), 93–100. https://doi.org/10.1016/S0269-7491(02)00411-6

Z. Fu, F. Wu, C. Mo, Q. Deng, W. Meng, J.P. Giesy, 2016. Comparison of arsenic and antimony biogeochemical behavior in water, soil and tailings from Xikuangshan, China. Sci. Total Environ. 539, 97–104. https://doi.org/10.1016/j.scitotenv.2015.08.146

J. Gál, A. Hursthouse, S. Cuthbert, 2007. Bioavailability of arsenic and antimony in soils from an abandoned mining area, Glendinning (SW Scotland). J. Environ. Sci. Health A, 42, 1263-1274. https://doi.org/10.1080/10934520701435585

P. Ganne, V. Cappuyns, A. Vervoort, L. Buve, R. Swennen, 2006. Leachability of heavy metals and arsenic from slags of metal extraction industry at Angleur (eastern Belgium). Science of the total environment, 356 (1), 69-85. https://doi.org/10.1016/j.scitotenv.2005.03.022

X. Guo, Z. Wu, M. He, X. Meng, X. Jin, N. Qiu, J. Zhang, 2014a. Adsorption of antimony onto iron oxyhydroxides: Adsorption behavior and surface structure. J. Hazard. Mater. 276,339-345.

X. Guo, K. Wang, M. He, Z. Liu, H. Yang, S. Li, 2014b. Antimony smelting process generating solid wastes and dust: characterization and leaching behaviors. J. Environ. Sci. 26, 1549-1556. https://doi.org/10.1016/j.jes.2014.05.022

C.S. Griggs, W.A. Martin, S.L. Larson, G. O'Connnor, G. Fabian, G. Zynda, D. Mackie, 2011. The effect of phosphate application on the mobility of antimony in firing range soils. Sci. Total Environ., 2397-2403. https://doi.org/10.1016/j.scitotenv.2011.02.043

J.P. Gustafsson. 2013. Visual MINTEQ. Version 3.1: a Windows Version of MINTEQA2, Version 3.1. Available on http://www2.lwr.kth.se/English/OurSoftware/vminteq/ (accessed on 27.05.2020)

T.H. Hasanin, T. Yamamoto, Y.Okamoto, S. Ishizaka S, Fujiwara T., 2016. A Flow Method for Chemiluminescence Determination of Antimony(III) and Antimony(V) Using a Rhodamine B-Cetyltrimethylammonium Chloride Reversed Micelle System Following On-Line Extraction. Anal Sci. 32(2), 245-50. https://doi.org/10.2116/analsci.32.245

M.C. He, 2007. Distribution and phytoavailability of antimony at an antimony mining and smelting area, Hunan, China. Environ. Geoch. Health 29, 209-219. https://doi.org/10.1007/s10653-006-9066-9

M.C. He, N.N. Wang, X.J. Long, C.J. Zhang, C.L. Ma, Q.Y. Zhong et al., 2019. Antimony speciation in the environment: recent advances in understanding the biogeochemical processes and ecological effects. J. Environ. Sci. 75, 14–39. https://doi.org/10.1016/j.jes.2018.05.023

Health Canada, 1999. Guidelines for Canadian Drinking Water Quality: Guideline Technical document – Antimony. 10 pp.

D.S.T. Hjortenkrans, N.S. Mansson, B.G. Bergback, A.V.Haggerud, 2009. Problems with Sb analysis of environmentally relevant samples. Environ. Chem., 6, 153-159. https://doi.org/10.1071/EN08077

X. Hu, X. Guo, M. He, S. Li, 2016. pH-dependent release characteristics of antimony and arsenic from typical antimony-bearing ores. J. Environ Sci., 44, 171-179. https://doi.org/10.1016/j.jes.2016.01.003

A.G. Ilgen, T.P. Trainor. 2012. Sb (III) and Sb (V) sorption onto Al-rich phases: hydrous Al oxide and clay minerals kaolinite KGa-1b and oxidized and reduced nontronite NAU-1. Environ. Sci. Technol., 46, 843-851. https://doi.org/10.1021/es203027v

S. Ishihara, H. Murakami, X. Li, 2011. Indium concentration in zinc ores in plutonic and volcanic environments. Examples at the Dulong and Dachang mines, South China. Bull. Geol. Surv. Japan 62, 259-272. https://doi.org/10.9795/bullgsj.62.259

S. Ishihara, P.T. Xuan, 2013. Distribution of Some Ore Metals around the Mau Due Stibnite Deposits, Northernmost Vietnam. Bull. Geol. Surv. Japan 64: 51–57. https://doi.org/10.9795/bullgsj.64.51

S.G. Johnston, W.W. Bennet, N. Dorian, K. Hockmann, N. Karimian, E.D. Burton, 2020. Antimony and arsenic speciation, redox-cycling and contrasting mobility in a mining-impacted river system. Science of The Total Environment, 710: 136354. https://doi.org/10.1016/j.scitotenv.2019.136354

Ľ. Jurkovič, J. Majzlan, E. Hiller, T. Klimko, B. Voleková-Lalinská, E. Hiller, P. Šottník, J. Göttlicher, R. Steininger, 2019. Natural attenuation of antimony and arsenic in soils at the abandoned Sb-deposit Poproč, Slovakia. Environ Earth Sci 78, 672. https://doi.org/10.1007/s12665-019-8701-6

W.R. Kammin, M.J. Brandt, 1988. ICP-OES evaluation of microwave digestion. Spectroscopy, 5(3), 49-55.

N. Karimian, S.G. Johnston, E.D. Burton, 2018. Iron and sulfur cycling in acid sulfate soil wetlands under dynamic redox conditions: A review. Chemosphere, 197: 803-816. https://doi.org/10.1016/j.chemosphere.2018.01.096

A.R. Kumar, P. Riyazuddin, 2007. Non-chromatographic hydride generation atomic spectrometric techniques for the speciation analysis of arsenic, antimony, selenium, and tellurium in water samples - a review Int. J. Environ. Anal. Chem. 87(7), 469-500. https://doi.org/10.1080/03067310601170415

C.R. Lehr, D.R. Kashyap, T.R. McDermott, 2007. New insights into microbial oxidation of antimony and arsenic. Appl. Environ. Microbiol.73, 2386–2389. https://doi: 10.1128/AEM.02789-06

A. Leuz, H. Monch, C.A. Johnson, 2006. Sorption of Sb (III) and Sb (V) to goethite: Influence on Sb (III) oxidation and mobilization. Environ. Sci. Technol. 40, 7277−7282. https://doi.org/10.1021/es061284b

K. Lewińska, A. Karczewska, M. Siepak, B.ernard Gałka; 2018. The Release of Antimony from Mine Dump Soils in the Presence and Absence of Forest Litter. Int. J. Environ Res. Public Health. 15(12), 2631. https://doi.org/10.3390/ijerph15122631

Li, W., Cook, N.J., Xie, G., C. L. Ciobanu, J-W. Li & Z.-Y. Zhang, 2018. Textures and trace element signatures of pyrite and arsenopyrite from the Gutaishan Au–Sb deposit, South China. Miner Deposita 54, 591–610. https://doi.org/10.1007/s00126-018-0826-0

778 P.C. Loni, M. Wu, W. Wang, H. Wang, L. Ma, C. Liu, Y. Song, H.T. O., 2020. Mechanism of microbial
779 dissolution and oxidation of antimony in stibnite under ambient conditions. J. Hazard. Mater. 385,
780 121561. https://doi.org/10.1016/j.jhazmat.2019.121561

781 J. Majzlan, M. Stevko, M., T. Lanczos, 2016. Soluble secondary minerals of antimony in Pezinok and
782 Kremnica (Slovakia) and the question of mobility or immobility of antimony in mine waters. Environ.
783 Chem. 13, 927–935. https://doi.org/10.1071/EN16013

784 E. Mariussen, 2012. Analysis of antimony (Sb) in environmental samples. Norwegian Defence
785 Research Establishment (FFI), 28 February 2012, 2 FFI-rapport 2012/00347, ISBN 978-82-464-2049-3,
786 27 pp.

787 K. Macgregor, G. MacKinnon, J.G. Farmer, M.C. Graham, 2015. Mobility of Antimony, Arsenic and
788 Lead at a Former Antimony Mine, Glendinning, Scotland. Sci.Total Environ. 529, 213–22.
789 https://doi.org/10.1016/j.scitotenv.2015.04.039

790 L. Mbadugha, D. Cowper, S. Dossanov, G.I. Paton, 2020. Geogenic and anthropogenic interactions at
791 a former Sb mine: environmental impacts of As and Sb. Environ. Geochem. Health.
792 https://doi.org/10.1007/s10653-020-00652-wS. Mitsunobu, T. Harad, Y. Takahashi, 2006.
793 Comparison of antimony behavior with that of arsenic under various soil redox conditions. Environ.
794 Sci. Technol. 40, 7270–7276. https://doi.org/10.1021/es060694x

795 R.S. Multani, T. Feldmann, G.P. Demopoulos, 2016. Antimony in the metallurgical industry: a review
796 of its chemistry and environmental stabilization options. Hydrometallurgy., 164, 141-153.
797 https://doi.org/10.1016/j.hydromet.2016.06.014

798 A.M. Murciego, A.G. Sanchez, M.A.R. Gonzalez, E.P. Gil, C.T. Gordillo, J.C. Fernandez, T.B. Triguero,
799 2007. Antimony distribution and mobility in topsoils and plants (Cytisus striatus, Cistus ladanifer and
800 Dittrichia viscosa) from polluted Sb-mining areas in Extremadura (Spain). Environ.Poll. 145, 15-21.
801 https://doi.org/10.1016/j.envpol.2006.04.004

802 Y.M. Nakamaru, F.J. Martín Peinado, 2017. Effect of soil organic matter on antimony bioavailability
803 after the remediation process. Environ. Pollut., 228, 425-432.
804 https://doi.org/10.1016/j.envpol.2017.05.042

805 M.J. Nash, J.E. Maskall, S.J. Hill, 2000. Methodologies for determination of antimony in terrestrial
806 environmental samples. J. Environ. Monit., 2, 97-109. https://doi.org/10.1039/a907875d

807 Z. Ning, T. Xiao, E. Xiao, 2015. Antimony in the Soil-Plant System in an Sb Mining/Smelting Area of
808 Southwest China. Int. J. Phytorem. 17(11), 1081-1089.
809 https://doi.org/10.1080/15226514.2015.1021955

810 G. Okkenhaug, Y.G. Zhu, L. Luo, M. Lei, X. Li, J. Mulder, 2011. Distribution, speciation and availability
811 of antimony (Sb) in soils and terrestrial plants from an active Sb mining area. Environ. Pollut., 159
812 (2011), 2427-2434. https://doi.org/10.1016/j.envpol.2011.06.028

813 G. Oprea, A. Michnea, C. Mihali, M. Senilă, C. Roman, S. Jelea, C. Butean, C. Barz, 2010. Arsenic and
814 Antimony Content in Soil and Plants from Baia Mare Area, Romania. Am. J. Environ. Sci. 6(1), 33-40.
815 https://doi.org/10.3844/ajessp.2010.33.40

C. Pérez-Sirvent, M.J. Martínez-Sánchez, S. Martínez-López, M. Hernández-Córdoba, 2011. Antimony distribution in soils and plants near an abandoned mining site. Microchem. J. 97, 52–5. https://doi.org/10.1016/j.microc.2010.05.009

A. Pierart, M. Shahid, N. Séjalon-Delmas, C. Dumat, 2015. Antimony Bioavailability: Knowledge and Research Perspectives for Sustainable Agricultures. J. Hazard. Mater. 289, 219–34. https://doi.org/10.1016/j.jhazmat.2015.02.011

B. Pahlavapour, M. Thompson, L. Thorne, 1980. Simultaneous determination of trace concentrations of arsenic, antimony and bismuth in soils and sediments by volatile hydride generation and inductively coupled plasma emission spectrometry. Analyst, 105, 756 -761. https://doi.org/10.1039/AN9800500756

J.-H. Park, S.-J. Kim, J.S. Ahn, D.-H. Lim, Y.-S. Han, 2018. Mobility of multiple heavy metalloids in contaminated soil under various redox conditions: effects of iron sulfide presence and phosphate competition. Chemosphere, 197, 344-352. https://doi.org/10.1016/j.chemosphere.2018.01.065

D.L. Parkhurst, C.A.J. Appelo, 1999. User's guide to PHREEQC (version 3) – a computer program for speciation, batch-reaction, one-dimensional transport and inverse geochemical calculations.

W. Qi, J. Cao, 1991. Background concentration of antimony in Chinese soils (In Chinese). Soil Bulletin 22, 209–210.

A.B. Radková, H.E. Jamieson, K.M. Campbell, 2020. Antimony mobility during the early stages of stibnite weathering in tailings at the Beaver Brook Sb deposit. Newfoundland. Appl. Geochem. 55, 104528. https://doi.org/10.1016/j.apgeochem.2020.104528

S. Rakshit, D. Sarkar, R. Datta. 2015. Surface complexation of antimony on kaolinite. Chemosphere, 119, 349-354. https://doi.org/10.1016/j.chemosphere.2014.06.070

A. J. Roper, P. A. Williams, and M. Fillela, 2012. 'Secondary Antimony Minerals: Phases That Control the Dispersion of Antimony in the Supergene Zone'. Chem.r Erde – Geochem.72, 9–14. https://doi.org/10.1016/j.chemer.2012.01.005

A. Rouwane, M. Rabiet, M. Grybos, G. Bernard, G. Gibaud, 2016. Effects of NO_3^- and PO_4^{3-} on the release of geogenic arsenic and antimony in agricultural wetland soil: a field and laboratory approach. Environ. Sci. Pollut. Res. 23, 4714–4728. https://doi.org/10.1007/s11356-015-5699-5

R. Salminen, M.J. Batista, M. Bidovec, A. Demetriades, B. De Vivo, W. De Vos, M. Duris, A. Gilucis, V. Gregorauskiene, J. Halamic, P. Heitzmann, A. Lima, G. Jordan, G. Klaver, P. Klein, J. Lis, J. Locutura, K. Marsina, A. Mazreku, P.J. O'Connor, S.Å. Olsson, R.-T. Ottesen, V. Petersell, J.A. Plant, S. Reeder, I. Salpeteur, H. Sandström, U. Siewers, A. Steenfelt, T. Tarvainen (2005) Geochemical Atlas of Europe. Part 1: Background Information, Methodology and Maps Geological Survey of Finland, Espoo (2005) (526 pages, 36 figures, 362 maps)

M.J. Serafimovska, S. Arpadjan, T. Stafilov, K. Tsekova, 2013. Study of the antimony species distribution in industrially contaminated soils. J. Soils Sed.13, 294–303. https://doi.org/10.1007/s11368-012-0623-9

T. Sh, C. Liu, C. Feng, 2012. Solubility, toxicity and sorption of antimony from smelter release. J. Geochem. Explor., 118, 14-18. https://doi.org/10.1016/j.gexplo.2012.03.007

Statista, 2019. Major countries in worldwide antimony mine production from 2015 to 2019 (in metric tons). Retrieved from https://www.statista.com/statistics/264958/antimony-production/ on 13 January 2020.

S. Steely, D. Amarasiriwardena, B. Xing, 2007. An investigation of inorganic antimony species and antimony associated with soil humic acid molar mass fractions in contaminated soils. Environ. Poll. 148, 590–598. https://doi.org/10.1016/j.envpol.2006.11.031

S. Sundar, J. Chakravarty, 2010. Antimony toxicity. Int. J. Environ. Res. Public Health 7(12), 4267-4277. https://doi.org/10.3390/ijerph7124267

K. Telford, W. Maher, F. Krikowa, S. Foster, 2008. Measurement of total antimony and antimony species in mine contaminated soils by ICPMS and HPLC-ICPMS. J. Environ. Monit., 10(1),136-140. https://doi.org/10.1039/B715465H

M. Tighe, P. Ashley, P. Lockwood, S. Wilson, 2005a. Soil, water and pasture enrichment of antimony and arsenic within a coastal floodplain system. Sci. Total Environ. 347 175–186. https://doi.org/10.1016/j.scitotenv.2004.12.008

M. Tighe, P. Lockwood, S. Wilson, 2005b. Adsorption of antimony(V) by floodplain soils, amorphous iron(III) hydroxide and humic acid. J. Environ. Monit.7 1177–1185. https://doi.org/10.1039/B508302H

M. Tighe, P. Lockwood, S. Wilson, L. Lisle, 2004. Comparison of digestion methods for ICP-OES analysis of a wide range of analytes in heavy metal contaminated soil samples with specific reference to arsenic and antimony. Comm. Soil Sci. Plant Anal. 35 (9–10), 1369–1385. http://dx.doi.org/10.1080/00103620701378441

USEPA, 2018. United States Environmental Protection Agency, 2018 Edition of the Drinking Water Standards and Health Advisories. Retrieved from: https://www.epa.gov/sites/production/files/2018-03/documents/dwtable2018.pdf (02.02.2020)

M. Verbeeck, R. Warrinnier, J.P. Gustafsson, Y. Thiry, E. Smolders, 2019. Soil organic matter increases antimonate mobility in soil: an Sb(OH)6 sorption and modelling study. Appl. Geochem. 104, 33-41. https://doi.org/10.1016/j.scitotenv.2020.138874

M. Verbeeck, Y. Thiry Y, E. Smolders, 2020a. Soil organic matter affects arsenic and antimony sorption in anaerobic soils. Environ Pollut. 257, 113566. https://doi.org/10.1016/j.envpol.2019.113566

M. Verbeeck, Thiry Y, E. Smolders, 2020b. Antimonate sorption in soils increases with ageing. Eur. J. Soil Sci. 71, 55–59. https://doi.org/10.1111/ejss.12845

V. Ettler, M. Mihaljevič , O. Šebek, Z. Nechutný, 2007. Antimony Availability in Highly Polluted Soils and Sediments – A Comparison of Single Extractions. Chemosphere 68 (3), 455–463. https://doi.org/10.1016/j.chemosphere.2006.12.085

D.H. Vu, X.M/ Biu, H.A. Le, 2012. The Effect of Mining Exploitation on Environment in Vietnam. China-ASEAN Mining Cooperation Forum and Exhibition 2012.

X. Wang, M. He, J. Xie et al. Heavy metal pollution of the world largest antimony mine-affected agricultural soils in Hunan province (China). J Soils Sediments 10, 827–837 (2010). https://doi.org/10.1007/s11368-010-0196-4

WHO, 2003. Antimony in Drinking-water Background document for development of WHO Guidelines for Drinking-water Quality. WHO/SDE/WSH/03.04/74, World Health Organization, Geneva, Switserland.

N.J. Wilson, D. Craw, K.A. Hunter, 2004. Antimony distribution and environmental mobility at an historic antimony smelter site, New Zealand. Environ. Pollut. 129, 257– 266. https://doi.org/10.1016/j.envpol.2003.10.014

S.C. Wilson, P.V. Lockwood, P.M. Ashley, M. Tighe, 2010. The chemistry and behaviour of antimony in the soil environment with comparisons to arsenic: a critical review. Environ. Pollut. 158; 1169-1181. https://doi.org/10.1016/j.envpol.2009.10.045

P.T. Xuan. 2011. Research on the influence of exploiting slag heaps and metal mineral processing on environment and human being health and put forward damage reducing methods (pp. 159-182). Vietnam Ministry of Science and Technology: Vietnam Academy of Science and Technology.

Y. Yuan, M. Xiang, C. Liu, B.K.G. Theng, 2017. Geochemical characteristics of heavy metal contamination induced by a sudden wastewater discharge from a smelter. J. Geochem. Explor. 176, 33-41. https://doi.org/10.1016/j.gexplo.2016.07.005

Figure and table captions

Figures

Figure 1 Representation of the sampling locations (aerial photographs from Google maps (2020), pictures from Le Thi Thuy Van).

Figure 1 Soluble Sb concentrations released from the slag (SL) and mine waste (SH) and soil (SO) samples with water (after 2 and 24 h of shaking) and with a 0.1 mol/l $Na_2HPO_4.2H_2O$ solution. Average ± standard deviation of 2 replicates. The number on top of each bar is the pH of the solution after extraction. For the soil samples, Sb concentrations obtained after the EN 12457-2 test were below detection limit.

Figure 2 Release of Sb as a function of pH from a mine waste (SH2), slag (SL1) and soil (SO1) sample. For comparison, the release of Sb with the $Na_2HPO_4.2H_2O$ 0.1 mol/l solution is also indicated. Average of two replicates. When error bars are not visible, they are smaller than the marker.

Figure 3 Comparison of the multi-acid digestion method and the $LiBO_2$ fusion for Sb and Fe. Average of 2 replicates

Figure 4 dissolved Sb concentrations as a function of pH : experimental and modelled results for (a) sample SH2 and (b) sample SL1

Tables

Table 1 Operational parameters of the different extractions

Table 2 Elemental composition of the samples investigated in this study. Trace elements were determined after multi-acid digestion; major elements were determined with $LiBO_2$ fusion.

Table 3 Antimony concentrations in soils impacted by mining and smelting activities reported in literature (non-limiting overview, in chronological order). The different digestion and analytical techniques are also given.

Figure 1

Click here to access/download;Figure;Figure1r.tif

Figure 2

Click here to access/download;Figure;Figure2r.tif

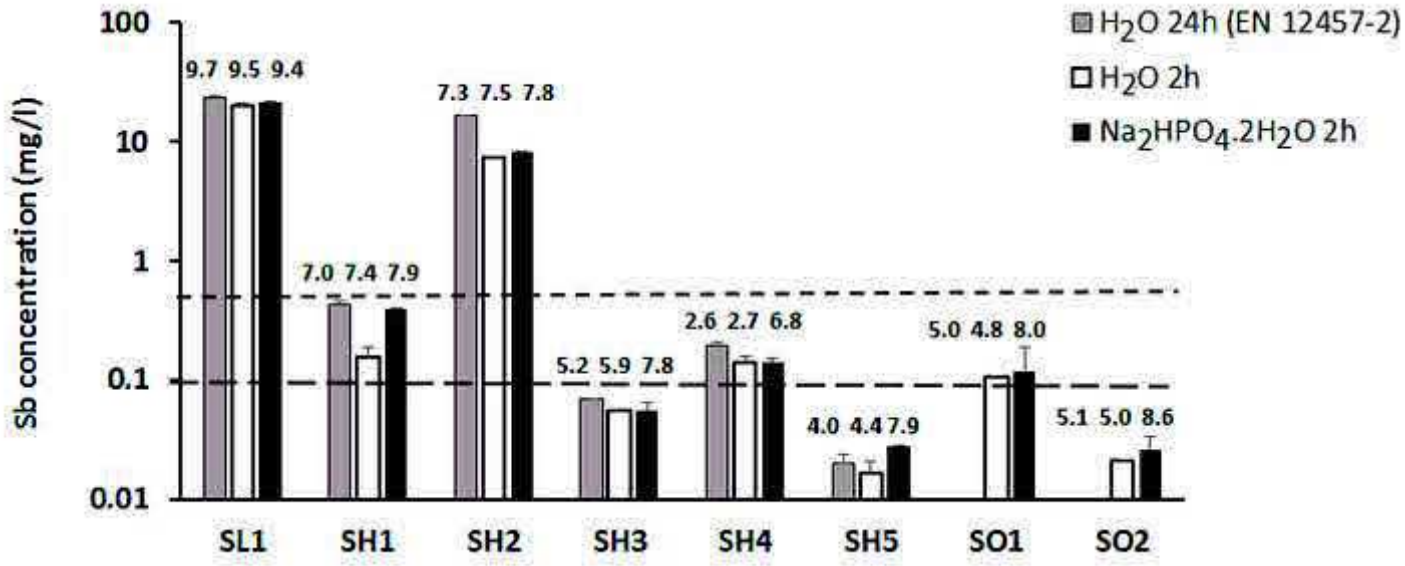

Figure 3

Click here to access/download;Figure;Figure3r.tif

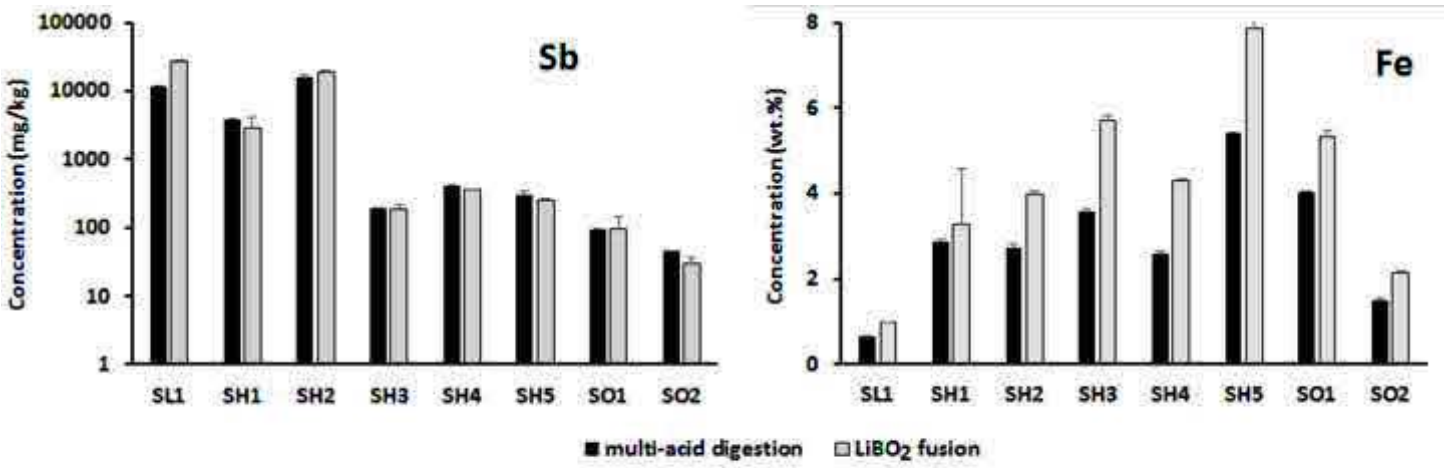

Figure 4

Click here to access/download;Figure;Figure4r.tif

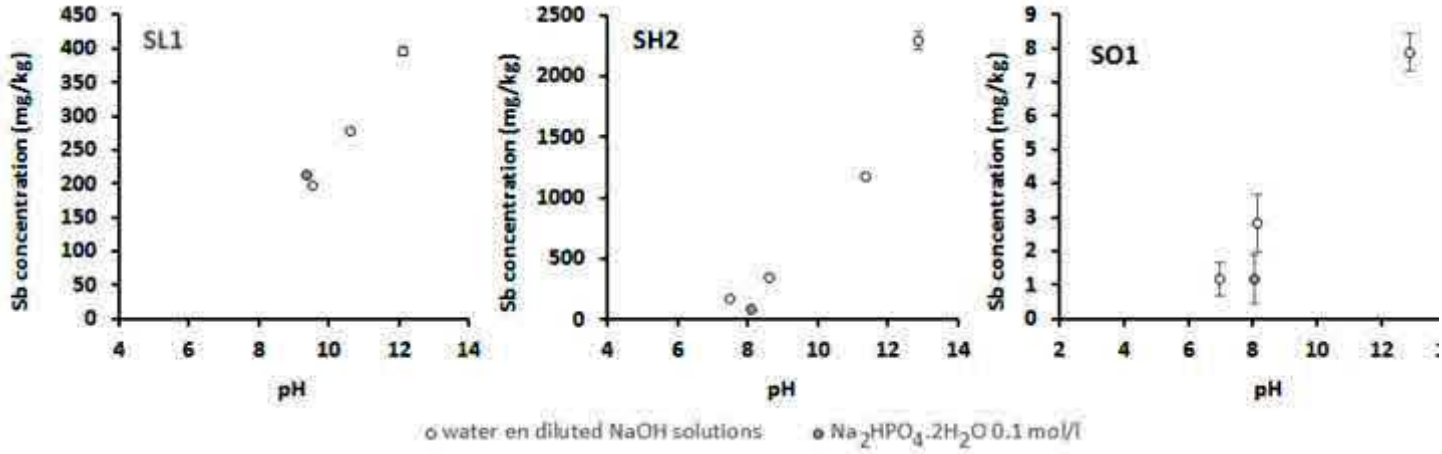

Figure 5

Click here to access/download;Figure;Figure5r.tif

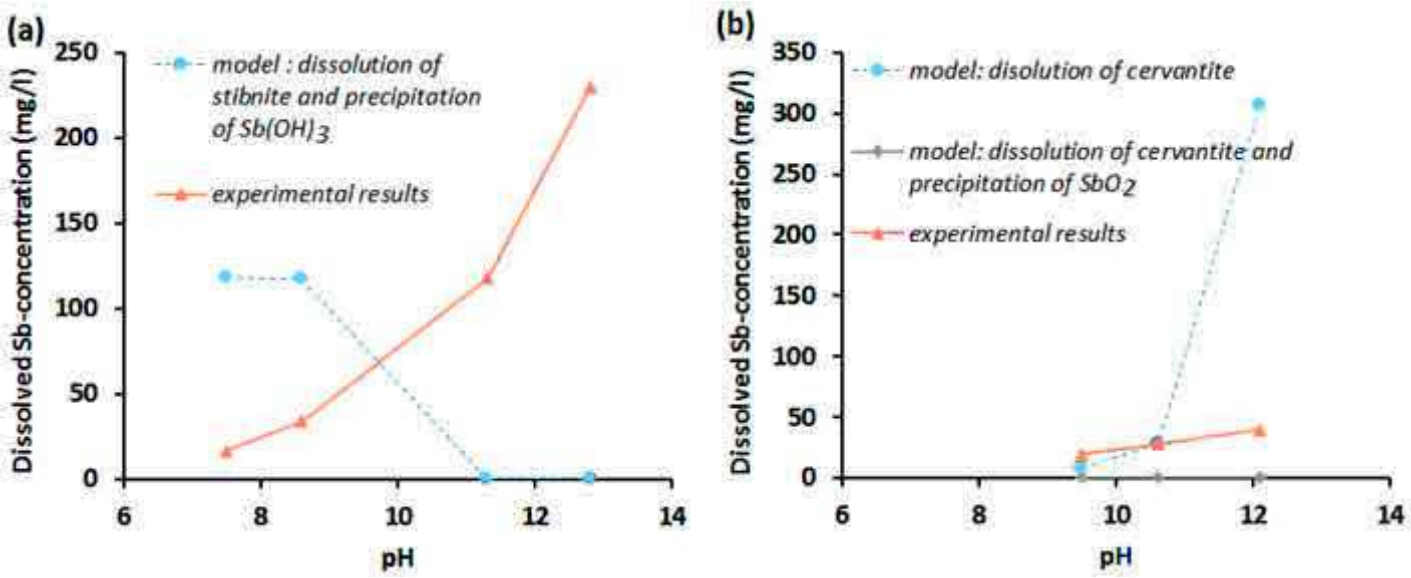

Table 1 *Operational parameters of the different extractions*

Extraction	**L/S ratio**	**Extraction time**	**Reference**
Demineralised water	10 l/kg	2 h	Ettler et al. (2007)
$Na_2HPO_4.2H_2O$ 0.1 mol/l	10 l/kg	2 h	Ettler et al. (2007)
NaOH 0.005, 0.01, and 0.1 mol/l	10 l/kg	24 h	This work
Demineralised water	10 l/kg	24 h	EN12457-2 (2002).

***Table** 2 Elemental composition of the samples investigated in this study. Trace elements were determined after multi-acid digestion; major elements were determined after $LiBO_2$ fusion.*

	As	Cd	Cr	Cu	Ni	Pb	Sb	Zn
	mg/kg	mg/kg	mg/kg	mg/kg	mg/kg	mg/kg	mg/kg	mg/kg
SH1	115 ± 3.3	9.0 ± 0.14	57 ± 0.1	124 ± 0.4	112 ± 1.5	31 ± 2.71	3785 ± 112	427 ± 107
SH2	130 ± 5.3	7.3 ± 0.44	88 ± 1.5	55 ± 4.6	95 ± 1.8	23 ± 1.34	15699 ± 1031	345 ± 17
SH3	167 ± 3.1	5.0 ± 1.43	141 ± 0.8	75 ± 10	91 ± 2.7	26 ± 0.76	191 ± 0.6	430 ± 100
SH4	114 ± 3.6	1.3 ± 0.04	59 ± 0.6	179 ± 7.4	65 ± 1.8	39 ± 0.93	407 ± 16	33 ± 1.6
SH5	54 ± 3.2	1.8 ± 0.16	116 ± 0.4	69 ± 0.2	55 ± 0.1	37 ± 0.43	299 ± 50	149 ± 1.0
SL1	10 ± 1.5	1.1 ± 0.14	26 ± 0.3	25 ± 1.3	19 ± 0.3	5 ± 0.02	11522 ± 317	115 ± 11
SO1	244 ± 1.0	1.0 ± 0.02	94 ± 1.1	41 ± 0.4	15 ± 0.9	21 ± 0.01	47 ± 13	36 ± 0.1
SO2	38 ± 0.6	0.4 ± 0.00	52 ± 4.9	23 ± 0.6	14 ± 0.7	22 ± 1.76	95 ± 1.7	26 ± 0.7

	Al	Ca	Fe	K	Mg	Si	S	pH
	wt.%	wt.%	wt.%	wt.%	wt.%	wt.%	mg/kg	
SH1	21.67 ± 0.91	2.20 ± 0.087	5.71 ± 0.11	5.06 ± 0.17	1.75 ± 0.13	28.0 ± 1.62	26500 ± 224	7.0 ± 0.01
SH2	17.58 ± 0.91	0.10 ± 0.003	4.30 ± 0.03	4.75 ± 0.21	1.27 ± 0.06	34.3 ± 1.48	34900 ± 1890	7.3 ± 0.05
SH3	19.11 ± 0.76	1.11 ± 0.049	7.87 ± 0.33	4.47 ± 0.17	2.23 ± 0.08	29.3 ± 1.00	22100 ± 537	5.2 ± 0.28
SH4	16.28 ± 0.52	0.02 ± 0.002	5.32 ± 0.14	2.82 ± 0.08	0.65 ± 0.02	35.6 ± 0.95	21700 ± 208	2.6 ± 0.02
SH5	18.97 ± 0.10	0.01 ± 0.003	2.15 ± 0.02	4.64 ± 0.05	1.06 ± 0.00	38.5 ± 0.72	8480 ± 40	4.0 ± 0.01
SL1	2.23 ± 0.00	3.21 ± 0.050	0.99 ± 0.01	0.31 ± 0.00	1.41 ± 0.03	44.1 ± 0.42	1550 ± 8	9.5 ± 0.02
SO1	5.70 ± 0.35	7.33 ± 2.65	3.26 ± 1.33	1.88 ± 0.83	4.33 ± 1.57	19.8 ± 6.99	97 ± 1	5.0 ± 0.07
SO2	11.92 ± 0.38	7.66 ± 0.14	3.99 ± 0.07	2.90 ± 0.07	4.21 ± 0.07	24.2 ± 0.64	47 ± 4	4.8 ± 0.15

Table 3 *Antimony concentrations in soils impacted by mining and smelting activities reported in literature (non-limiting overview, in chronological order). The different digestion and analytical techniques are also given.*

Location	Source of Sb	Sb concentration in soil	Method of analysis	reference
Soils around five historic mining areas in the UK	Mining area (Cu, Pb, Zn, As, and Sb)	0.5-40.6 mg/kg	HG-FAAS analysis after digestion with $HClO_4$, HNO_3, HCl	Flynn et al. (2003)
Forests and tilled soils, Prıbram, Czech Republic	Mining, Sb mineralisation in Pb-Ag-Zn mineralization	7.72-705 mg/kg	ICP-MS analysis after acid digestion with $HClO_4$/HF	Ettler et a. (2007)
Soils in and around the mining area, Glendinning, Scotland	Mining, polymetallic mineralisation including stibnite	14.0–673 mg/kg 10.3-1200 mg/kg	ICP-AES analysis after microwave Aqua Regia destruction	Gal et al. (2007)
Topsoils, Extremadura, Spain	Sb-mining area	14.3-5180 mg/kg	INAA	Murciego et al. (2007).
Soils from a mining site, Hunan, southwest China	Xikuangshan Sb mine	10-2159 mg/kg	AFS analysis after Aqua Regia digestion	Wang (2009)
Garden and Industrial soils, Baia Mare, Romania	Area contaminated by dust from metallurgical plants	0.85-40.06 mg/kg	ICP-AES analysis after hotplate Aqua Regia destruction	Oprea et al (2010)
Soil samples (B horizon) in the vicinity of the Bayley Park Sb prospect near Armidale, NSW, Australia	Sb-mineralisation area (no mining)	Up to 150 mg/kg	Not mentioned	Diemar et al. (2009)
Technosols with pH values of 3.5–7.0 Poproč, Slovakia	abandoned Sb-deposit Poproč	13.4-5757 mg/kg	ICP-OES and ICP-MS analysis after acid digestion	Jurkovic et al. (2010)
Soils from Sierra Minera, Murcia, Spain		5-40 mg/kg	HG-AFS analysis after microwave digestion with HF/HNO_3	Pérez-Sirvent et al. (2011)
Soils from a mining site Xikuangshan, southwest China	Active Sb mining area	527-11798 mg/kg	HG-ICP-OES analysis after closed microwave HNO_3/HF digestion	Okkenhaug et al. (2011)
Agricultural soils, Zamora, Spain	Mining, hydrothermal Pb–Sb–Ag-rich deposit	14.1–324 mg/kg	ICP-AES analysis after microwave Aqua Regia destruction	Álvarez-Ayuso et al. (2012)
Industrially polluted areas in Bulgaria end Macedonia		2.5 – 105 mg/kg	ETAAS analysis after hot plate digestion with HNO_3/HCl/HF	Serafimovska et al. (2013)
Soils from an abandoned mine, Sardinia, Italy	Su Suergiu the antimony deposit	<8 – 4400 mg/kg	ICP-MS analysis after microwave digestion with H_2O_2/ HF/HCl/ HNO_3/	Cidu et al. (2014)
Soils from close to the spoil heap, Glendinning mine, SW Scotland	Former Sb mine	6.77-261 mg/kg	ICP-OES analysis after ashing and HF/HNO_3 digestion	Mcgregor et al. (2015)
Soils from a mining site, Hunan, southwest China	Banpo Sb mine	267-5633 mg/kg	ICP-MS analysis after acid digestion with HNO_3/HF	Ning et al. (2015)
Soils in the vicinity of smelter, Xikuangshan Hunan, southwest China	Xikuangshan mining area	3.23-6946 mg/kg	HG-AFS after digestion with HNO_3/HF/H_2SO_4	Fu et al. (2016)
Soils in and around the mining area, Glendinning, Scotland	Mining, polymetallic mineralisation including stibnite	108 - 15490 mg/kg	ICP-MS analysis after HNO_3 and H_2O_2 digestion	Mbadugha et al. (2020)

AFS = atomic fluorescence spectrometry, HG = hydride generation, ICP = induced coupled plasma, ETAAS = Electrothermal Atomic Absorption Spectrometry, FAAS = Flame Atomic absorption spectroscopy, MS = mass spectrometry, INAA = Instrumental Neutron Activation Analysis, OES = optical emission spectrometry